Supplementary Information

CHEMICAL AND PHOTOCHEMICAL PROPERTIES OF CHLOROHARMINE DERIVATIVES IN AQUEOUS SOLUTIONS

Federico A. O. Rasse-Suriani[a,‡], *M. Paula Denofrio*[a,‡], *Juan G. Yañuk*[a], *M. Micaela Gonzalez*[a], *Ezequiel Wolcan*[b], *Marco Seifermann*[c], *Rosa Erra-Balsells*[d,*] *and Franco M. Cabrerizo*[a,*]

[a] Instituto de Investigaciones Biotecnológicas - Instituto Tecnológico de Chascomús (IIB-INTECH), Universidad Nacional de San Martín (UNSAM) - Consejo Nacional de Investigaciones Científicas y Técnicas (CONICET), Intendente Marino Km 8.2, CC 164 (B7130IWA), Chascomús, Argentina. E-mail: fcabrerizo@intech.gov.ar

[b] Instituto de Investigaciones Fisicoquímicas Teóricas y Aplicadas (INIFTA, UNLP, CCT La Plata-CONICET), Diag. 113 y 64, Sucursal 4, C.C. 16, (B1906ZAA) La Plata, Argentina.

[c] Institute of Pharmacy and Biochemistry, University of Mainz, Staudingerweg 5, Mainz, Germany.

[d] CIHIDECAR - CONICET, Departamento de Química Orgánica, Facultad de Ciencias Exactas y Naturales, Universidad de Buenos Aires, Pabellón 2, 3p, Ciudad Universitaria, (1428) Buenos Aires, Argentina. E-mail: erra@qo.fcen.uba.ar

‡ These authors contributed equally.

* To whom correspondence should be addressed (fcabrerizo@intech.gov.ar and erra@qo.fcen.uba.ar)

Contents: **Page**

1. Spectrophotometric titration of 6-chloroharmine (6-Cl-Ha)

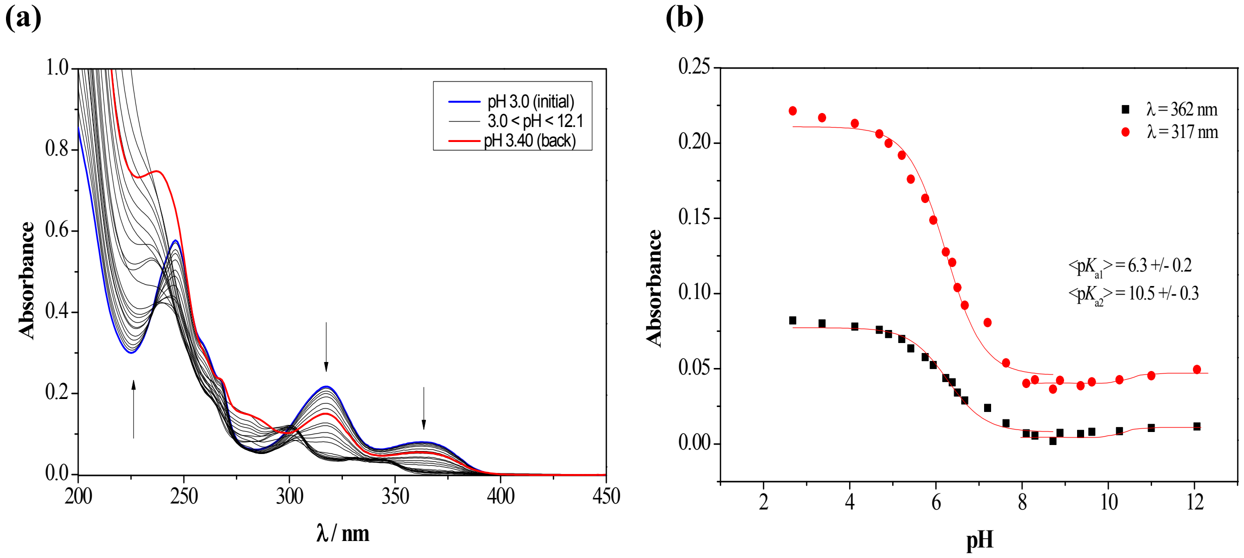

Figure ESI.1. (a) Evolution of the UV-vis absorption spectra of 6-Cl-Ha (10 µM) as a function of the pH (black lines). Spectrum in blue, called “initial”, corresponds to the initial acidic solution (pH 3.0). Spectrum in red, called “back”, corresponds to 6-Cl-Ha aqueous solution that was acidify (pH 3.4) after alkali treatment (pH 12.1) **(b)** Spectrophotometric titration curve depicted at two different wavelengths.

2. Spectrophotometric titration of 8-chloroharmine (8-Cl-Ha)

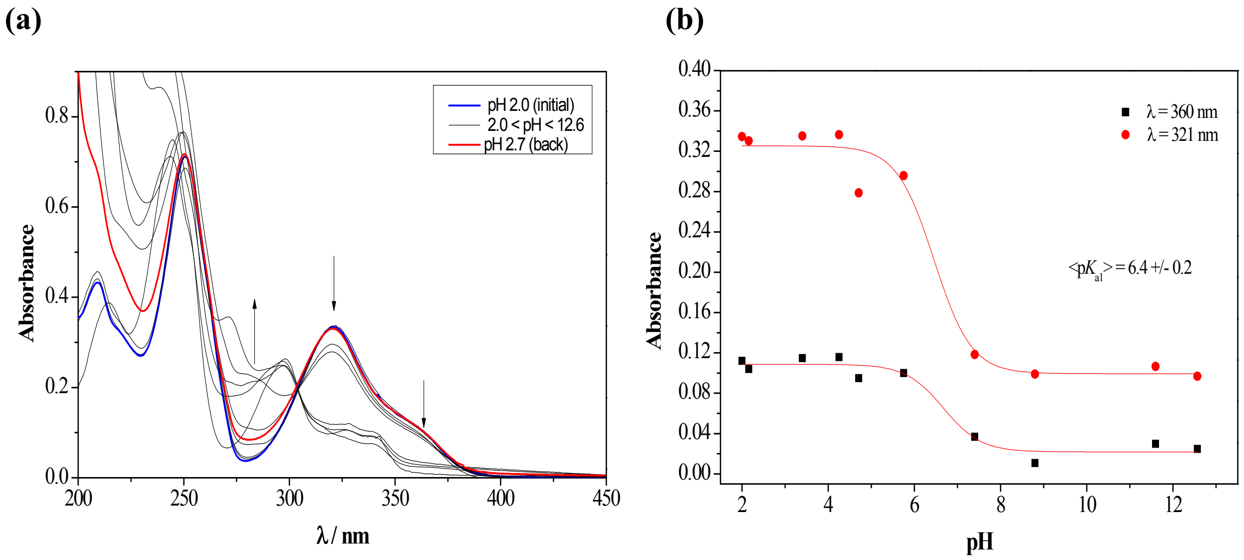

Figure ESI.2. (a) Evolution of the UV-vis absorption spectra of 8-Cl-Ha (20 µM) as a function of the pH (black lines). Spectrum in blue, called "initial", corresponds to the initial acidic solution (pH 2.0). The red line, called "back", represents the spectrum of 8-Cl-Ha aqueous solution that was acidify (pH 2.7) after alkali treatment (pH 12.6) **(b)** Spectrophotometric titration curve depicted at two different wavelengths.

3. Spectrophotometric titration of 6,8-dichloroharmine (6,8-diCl-Ha)

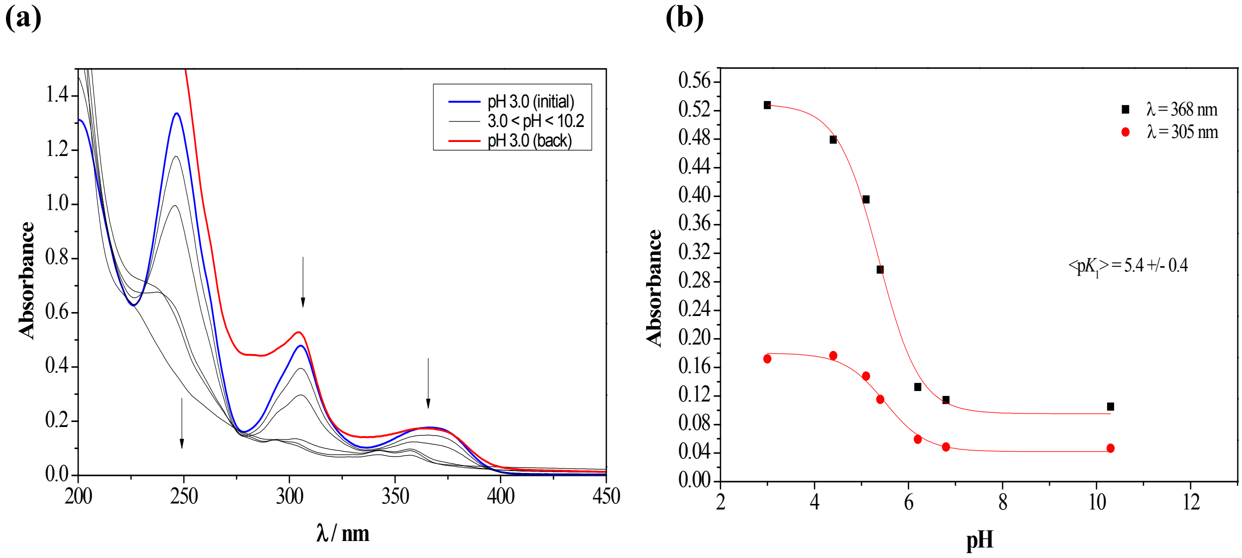

Figure ESI.3. **(a)** Evolution of the UV-vis absorption spectra of 6,8-diCl-Ha (20 µM) as a function of the pH (black lines). Spectrum in blue, called "initial", corresponds to the initial acidic solution (pH 3.0). Spectrum in red, called "back", corresponds to 6,8-diCl-Ha aqueous solution that was acidify (pH 3.0) after alkali treatment (pH 10.2) **(b)** Spectrophotometric titration curve depicted at two different wavelengths.

4. Thermal stability of chloroharmine derivatives under acidic and alkaline conditions

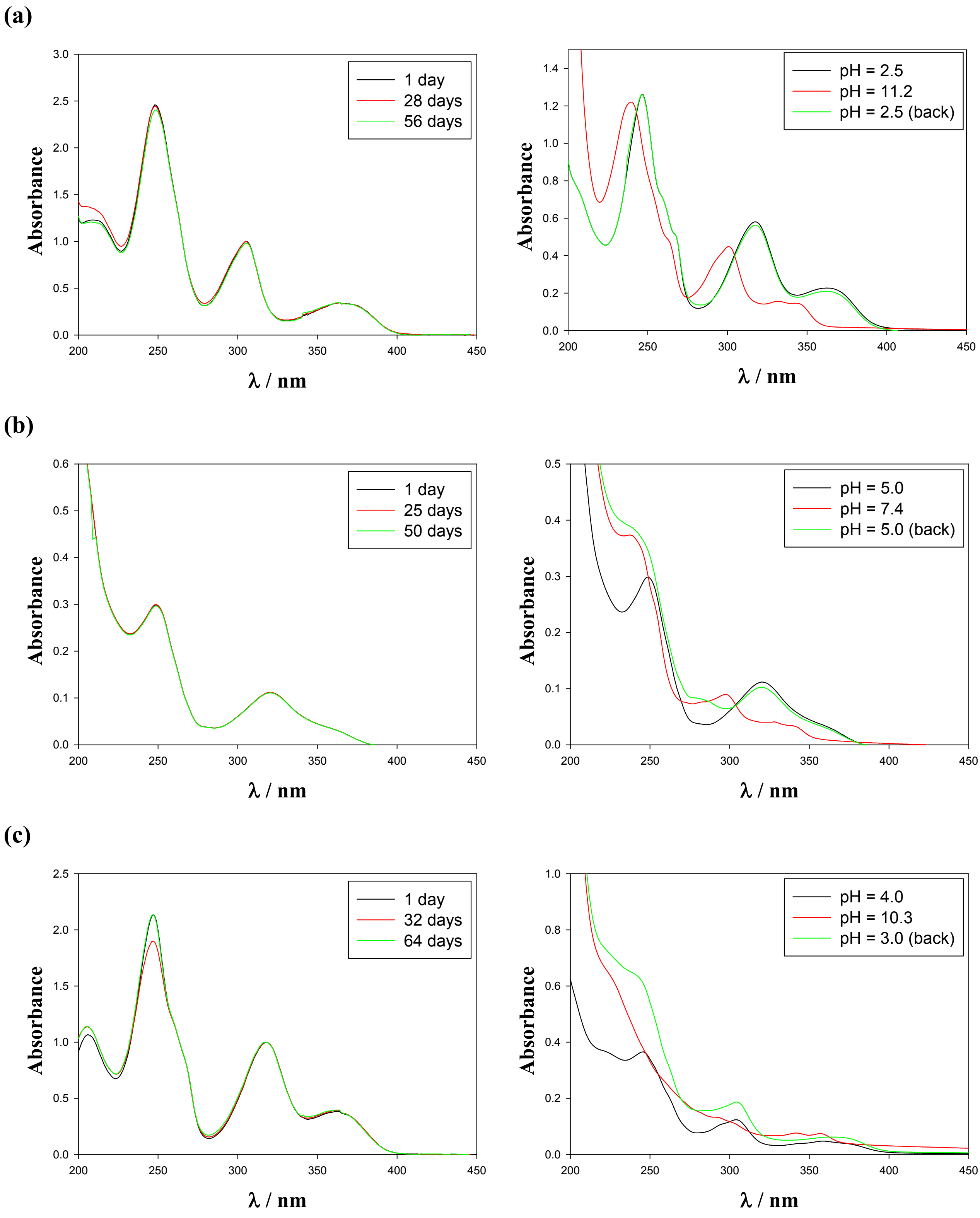

Figure ESI.4. UV-vis absorption spectra of **(a)** 6-Cl-Ha, **(b)** 8-Cl-Ha and **(c)** 6,8-diCl-Ha. *Left column*: spectra of acidic aqueous solutions storage in the dark for more than 50 days. *Right column*: spectra of acidic (black) and alkaline (red) chloroharmine solutions. Green lines show the spectra “back” of chloroharmines that were acidify (pH 2.5, 5.0 and 3.0, respectively) after alkali treatment (pH 11.2, 7.4 and 10.3, respectively).

5. **Table ESI.1:** Composition (% character) of relevant Molecular Orbitals of chloroharmine derivatives (see text for details).

Molecule	**MO**	**Percentage contribution of each fragment to MO**							
		N/NH$^+$ (Pyridine ring)	**NH (Pyrrolic ring)**	**6-Cl**	**8-Cl**	**CH$_3$**	**O-CH$_3$**	**Phenyl ring**	**Pyridine ring**
6-Cl-Ha	H–1	6.0	2.7	1.4		0.4	14.8	49.6	25.1
	H	1.2	19.9	6.5		1.5	0.8	37.7	32.4
	L	11	0.4	0.6		1.6	2.4	45.9	38.0
	L+1	0.9	1.8	3.4		3.9	0.8	54.8	34.3
8-Cl-Ha	H–1	6.3	3.6		0.5	0.4	12.8	58.3	18.2
	H	0.9	18.9		5.5	1.5	3.8	33.3	36.1
	L	11.3	0.6		1.2	1.7	2.1	44.9	38.1
	L+1	0.8	1.4		1.4	3.6	0.6	44.7	47.6
6-Cl-HaH$^+$	H–1	2.3	14.3	0.6		1.3	10.0	47.0	24.4
	H	3.0	7.1	11.6		0.1	8.6	55.2	14.4
	L	13.4	1.6	0.3		2.8	2.5	26.7	52.7
	L+1	2.7	2.2	0.9		2.4	0.2	15.5	76.1
8-Cl-HaH$^+$	H–1	1.3	18.4		2.8	0.8	1.4	53.2	22.2
	H	3.7	2.5		8.0	0.5	19.1	52.5	13.8
	L	13.5	1.8		0.3	2.9	2.6	26.0	52.9
	L+1	2.8	2.4		0.3	2.2	0.2	15.2	76.8
6,8-diCl-Ha	H–1	8.4	0.6	3.2	1.7	0.1	6.5	56.5	23.0
	H	0.6	20.9	5.0	3.0	1.7	0.0	32.6	36.2
	L	10.3	0.9	0.2	1.8	1.4	1.3	50.6	33.6
	L+1	0.6	2.1	3.9	1.1	2.6	0.8	58.9	30.0
6,8-diCl-HaH$^+$	H–1	3.8	1.6	2.2	6.1	0.4	19.3	52.9	13.8
	H	0.7	17.4	10.8	3.8	0.7	0.2	47.6	18.7
	L	13.2	1.8	0.2	0.5	2.7	2.3	28.5	51.0
	L+1	2.5	2.0	1.2	0.5	2.4	0.2	19.8	71.6

6. Experimental and calculated electronic spectra of 8-Cl-Ha and 8-Cl-HaH$^+$

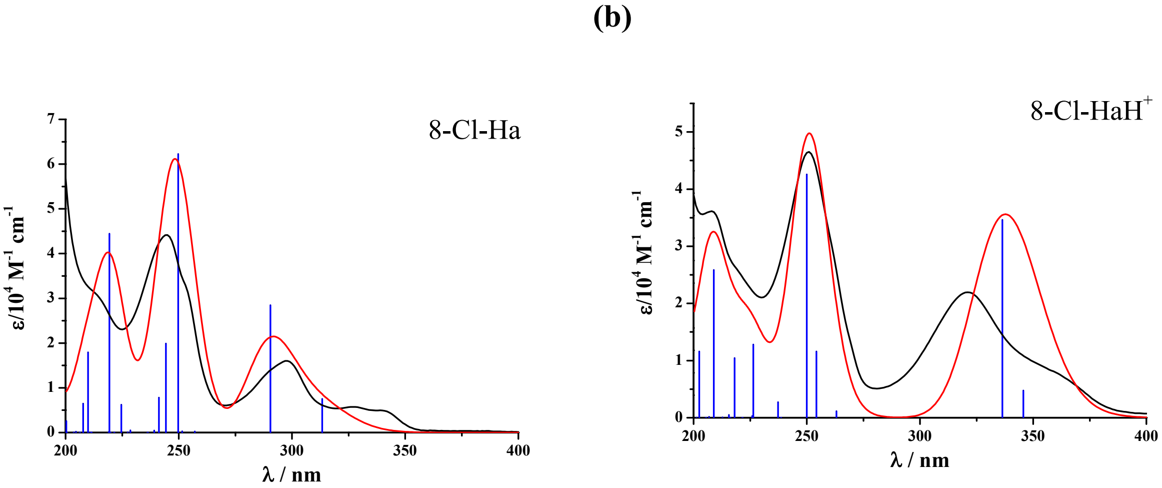

Figure ESI.5. Comparison of the UV-vis absorption spectrum (black lines) with TD-DFT calculated electronic transitions (blue lines) and simulated spectra (red lines) for **(a)** 8-Cl-Ha and **(b)** 8-Cl-HaH$^+$. The vertical transition energies were calculated at the optimized ground-state geometry by TD-DFT using B3LYP hybrid functional and aug-cc-pVDZ basis set including solvent effects (water) through the Polarizable Continuum Model. See text for details.

7. Experimental and calculated electronic spectra of 6,8-diCl-Ha and 6,8-diCl-HaH$^+$

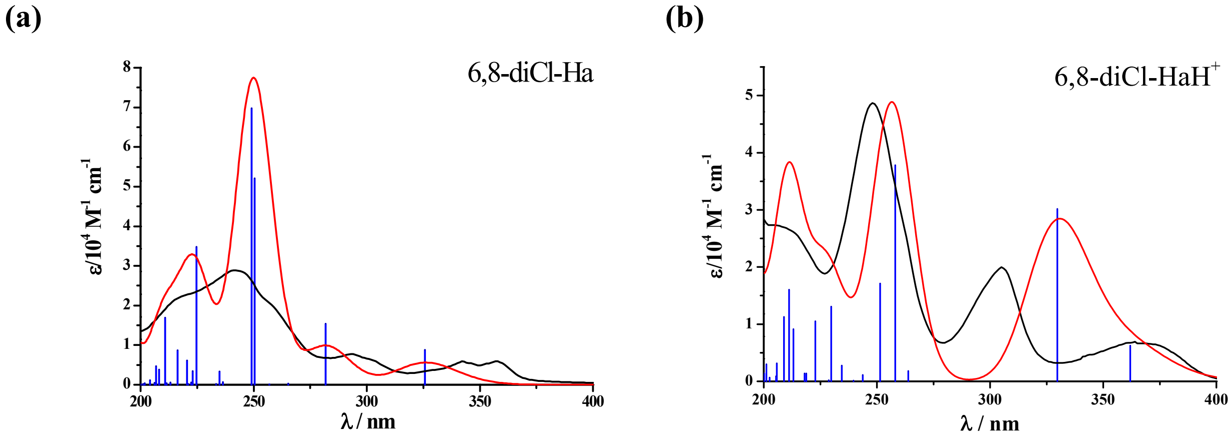

Figure ESI.6. Comparison of the UV-vis absorption spectrum (black lines) with TD-DFT calculated electronic transitions (blue lines) and simulated spectra (red lines) for **(a)** 6,8-diCl-Ha and **(b)** 6,8-diCl-HaH$^+$. The vertical transition energies were calculated at the optimized ground-state geometry by TD-DFT using B3LYP hybrid functional and aug-cc-pVDZ basis set including solvent effects (water) through the Polarizable Continuum Model. See text for details.

8. Triplet state kinetics

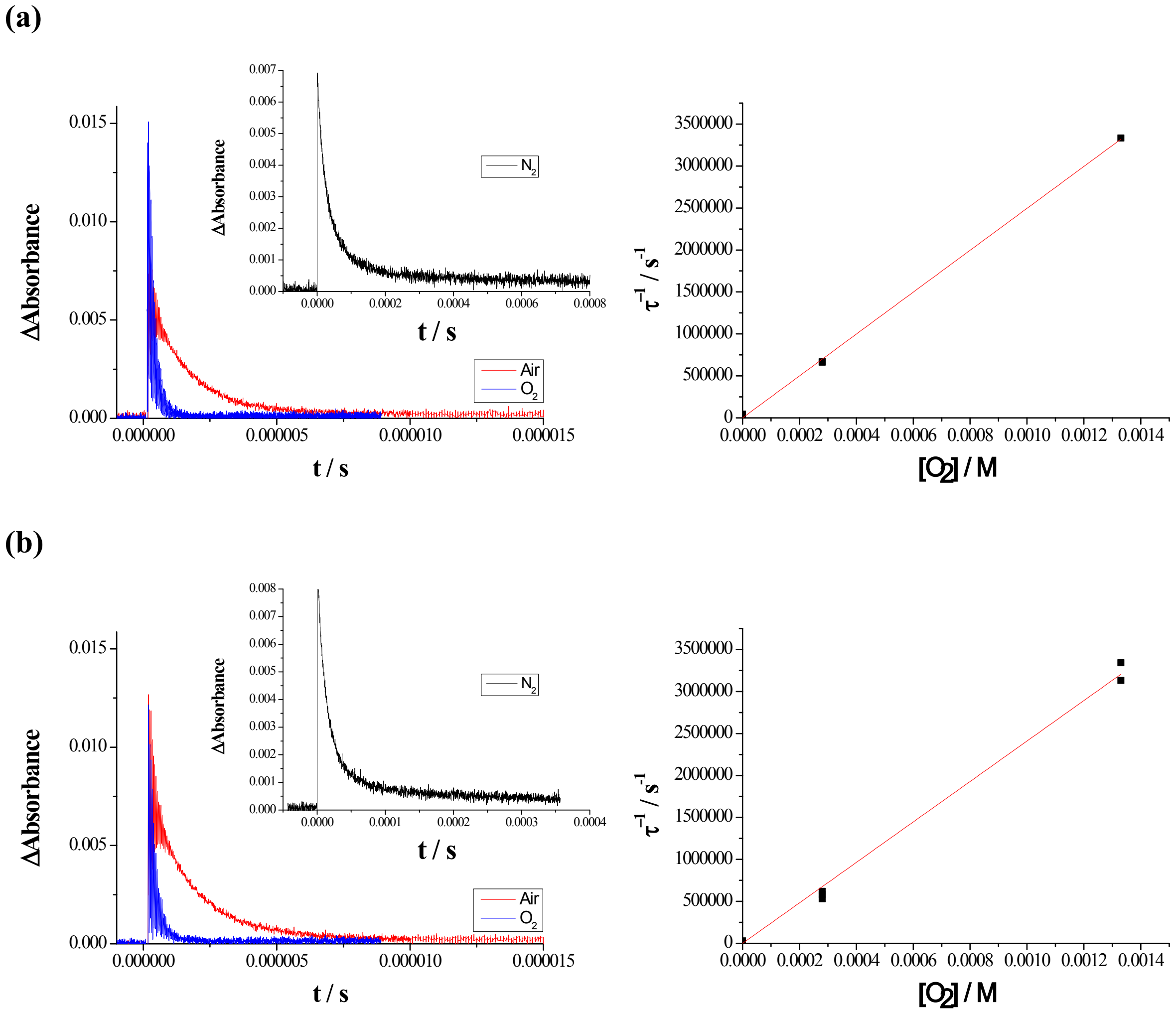

Figure ESI.7. *Left column*: kinetic traces obtained in a time-resolved triplet state absorption experiment of **(a)** 8-Cl-HaH$^+$ and **(b)** 6,8-diCl-HaH$^+$, in H_2O at pH 4. Data are shown for N_2-saturated (*inset*), air-equilibrated and O_2-saturated samples. *Right column*: Plot of the first-order rate constant for the decay of the triplet state against the dissolved oxygen concentration. The slope yields a rate constant for O_2 quenching of the triplet state of **(a)** 8-Cl-HaH$^+$ and **(b)** 6,8-diCl-HaH$^+$ of $(2.49 \pm 0.3) \times 10^9$ M^{-1} s^{-1} and $(2.41 \pm 0.2) \times 10^9$ M^{-1} s^{-1}, respectively.

9. Evolution of the βCs and H_2O_2 concentrations in irradiated air-equilibrated aqueous solutions.

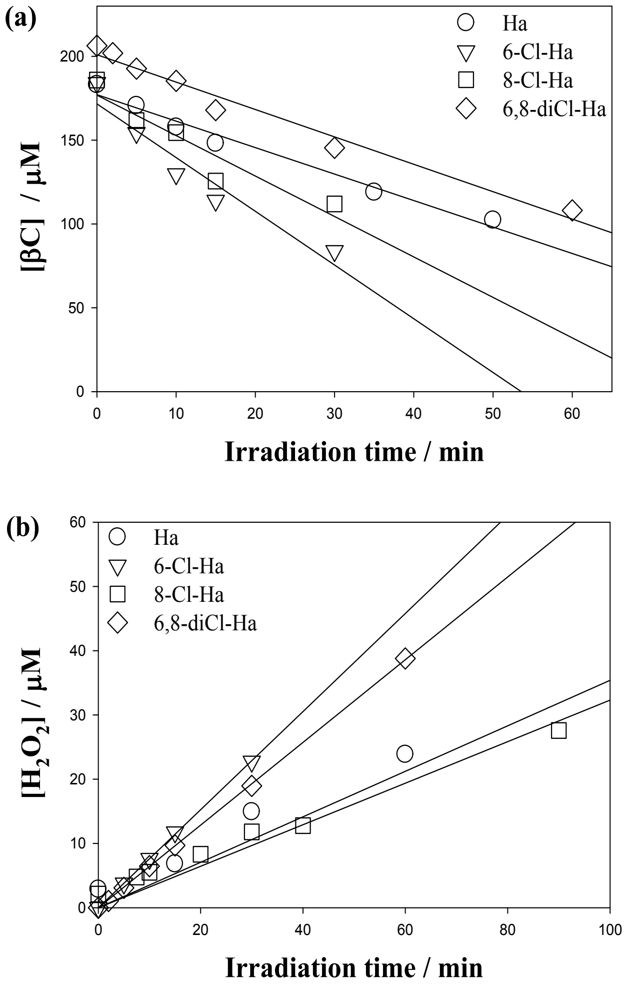

Figure ESI.8. Evolution of **(a)** βC ($[\beta C]_0 = 180$ μM) and **(b)** H_2O_2 concentration in air-equilibrated acidic (pH 4.0) aqueous solutions as a function of the elapsed 350 nm irradiation time. βC concentrations were assessed using HPLC analysis.

10. Comparative analysis of the effect of HCl and HClO$_4$ on the photodegradation of 6-Cl-HaH$^+$.

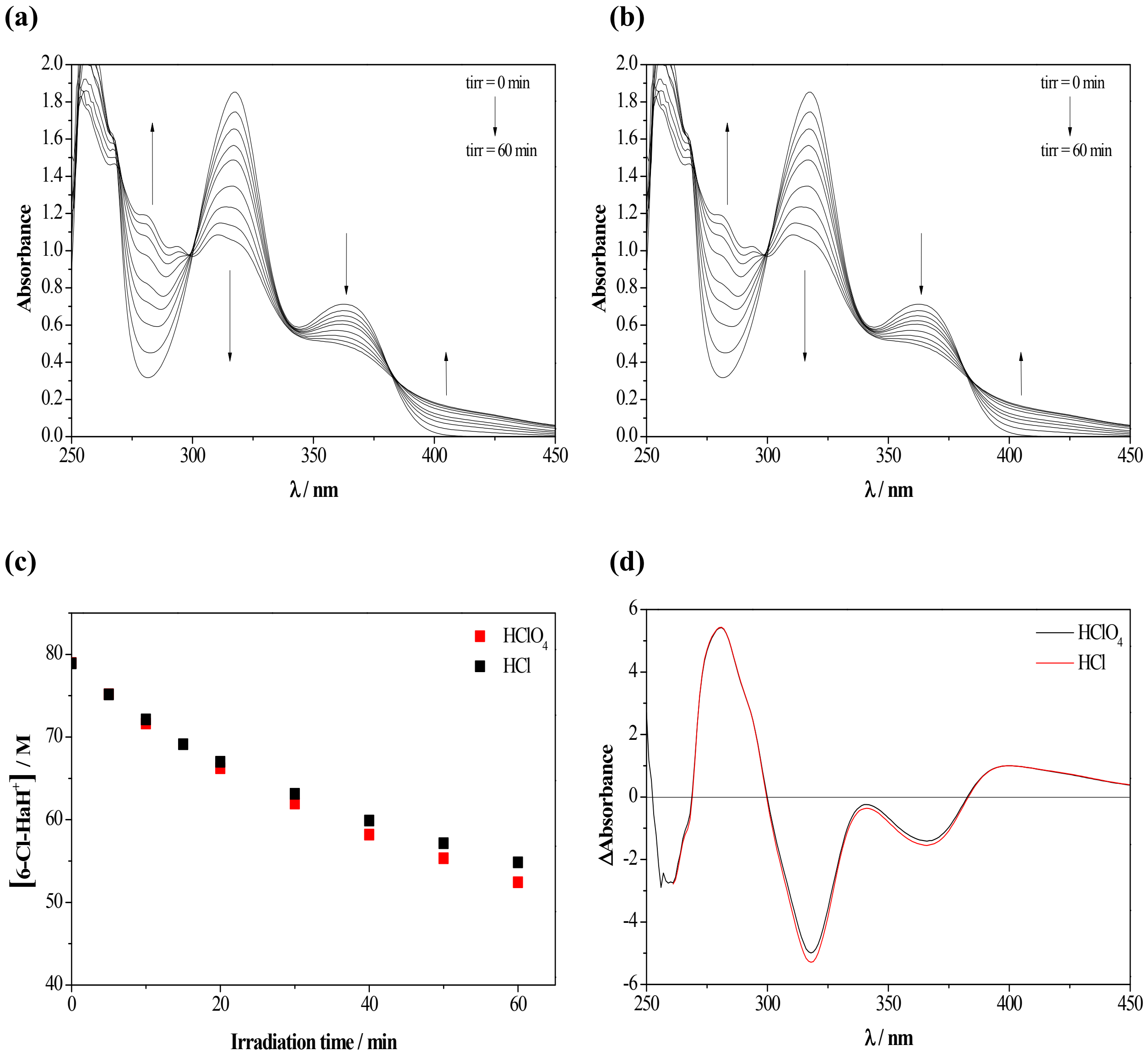

Figure ESI.9. **(a)** and **(b)** show the evolution of the UV-vis spectra of air-equilibrated acidic 6-Cl-HaH$^+$ ([βC]$_0$ = 80 µM, pH 4.0) aqueous solutions as a function of irradiation time when HCl and HClO$_4$ were used to fix the pH of 6-Cl-HaH$^+$ solutions, respectively. **(c)** Comparative kinetics. **(d)** Normalized (at 400 nm) Experimental Difference (NED) spectra.

11. Evolution of the βCs (6-Cl-HaH$^+$) and H_2O_2 concentrations in irradiated air-equilibrated aqueous solutions in the presence of ROS scavengers.

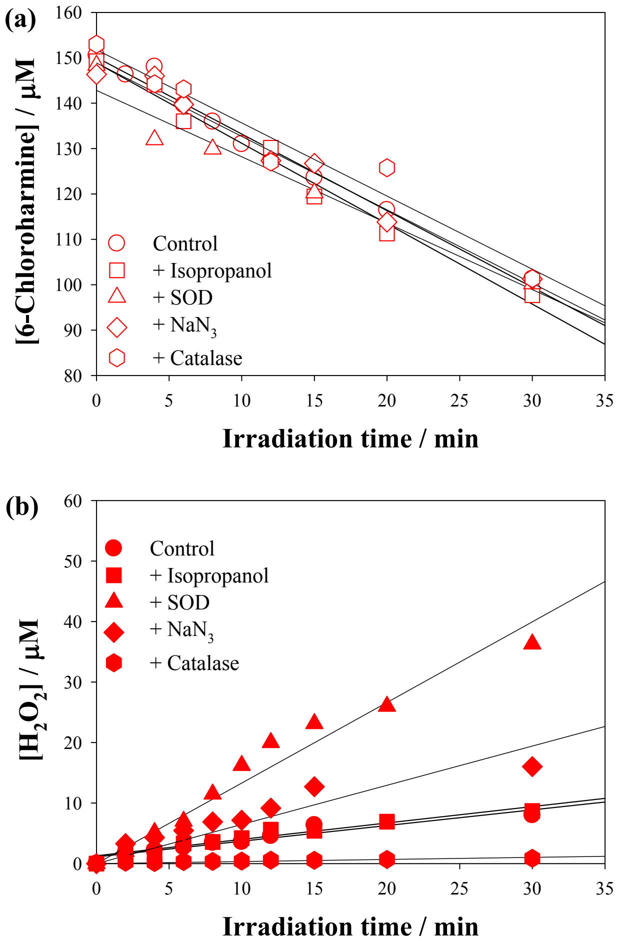

Figure ES.10. Evolution of **(a)** protonated 6-chloroharmine (6-Cl-HaH$^+$) and **(b)** H_2O_2 concentration in air-equilibrated aqueous solutions as a function of irradiation time in the presence of different ROS scavengers. Experiments performed at pH 4.0, 6-Cl-HaH$^+$ (150 µM).